



STUDY OF AN AQUEOUS LITHIUM CHLORIDE DESICCANT SYSTEM: AIR DEHUMIDIFICATION AND DESICCANT REGENERATION

NELSON FUMO* and D. Y. GOSWAMI**[†]

*Universidad Nacional Experimental del Táchira, San Cristóbal, Venezuela

**Solar Energy and Energy Conversion Laboratory, Department of Mechanical Engineering, University of Florida, POB 11630, Gainesville, FL 32611-6300, USA

Received 3 November 2000; revised version accepted 27 December 2001

Communicated by BYARD WOOD

Abstract—Desiccant systems have been proposed as energy saving alternatives to vapor compression air conditioning for handling the latent load. Use of liquid desiccants offers several design and performance advantages over solid desiccants, especially when solar energy is used for regeneration. For liquid–gas contact, packed towers with low pressure drop provide good heat and mass transfer characteristics for compact designs. This paper presents the results from a study of the performance of a packed tower absorber and regenerator for an aqueous lithium chloride desiccant dehumidification system. The rates of dehumidification and regeneration, as well as the effectiveness of the dehumidification and regeneration processes were assessed under the effects of variables such as air and desiccant flow rates, air temperature and humidity, and desiccant temperature and concentration. A variation of the Öberg and Goswami mathematical model was used to predict the experimental findings giving satisfactory results. © 2002 Elsevier Science Ltd. All rights reserved.

1. INTRODUCTION AND BACKGROUND

Liquid desiccant cooling systems have been proposed as alternatives to the conventional vapor compression cooling systems to control air humidity, especially in hot and humid areas. Research has shown that a liquid desiccant cooling system can reduce the overall energy consumption, as well as shift the energy use away from electricity and toward renewable and cheaper fuels (Öberg and Goswami, 1998a). Burns *et al.* (1985) found that utilizing desiccant cooling in a supermarket reduced the energy cost of air conditioning by 60% as compared to conventional cooling. Öberg and Goswami (1998a) modeled a hybrid solar cooling system obtaining an electrical energy savings of 80%, and Chengchao and Ketao (1997) showed by computer simulation that solar liquid desiccant air conditioning has advantages over vapor compression air conditioning system in its suitability for hot and humid areas and high air flow rates.

Use of liquid desiccants offers several design and performance advantages over solid desiccants, especially when solar energy is used for regeneration (Öberg and Goswami, 1998c). Several liquid

desiccants are commercially available: triethylene glycol, diethylene glycol, ethylene glycol, and brines such as calcium chloride, lithium chloride, lithium bromide, and calcium bromide which are used singly or in combination. The usefulness of a particular liquid desiccant depends upon the application. At the University of Florida, Öberg and Goswami (1998a,b) conducted a study of a hybrid solar liquid desiccant cooling system using triethylene glycol (TEG) as the desiccant. Their experimental work concluded that glycol works well as a desiccant. However, pure triethylene glycol does have a small vapor pressure which causes some of the glycol to evaporate into the air. Although triethylene glycol is nontoxic, any evaporation into the supply air stream makes it unacceptable for use in air conditioning of an occupied building. Therefore, there is a need to evaluate other liquid desiccants for hybrid solar desiccant cooling systems. Lithium chloride (LiCl) is a good candidate material since it has good desiccant characteristics and does not vaporize in air at ambient conditions. A disadvantage with LiCl is that it is corrosive. This paper presents an experimental and theoretical study of aqueous lithium chloride as a desiccant for a solar hybrid cooling system, using a packed bed dehumidifier and regenerator.

A number of experimental studies have been carried out on packed bed dehumidifiers using salt

[†] Author to whom correspondence should be addressed. Tel.: +1-352-392-0812; fax: +1-352-392-1071; e-mail: solar@cimar.me.ufl.edu

solutions as desiccants. Chung *et al.* (1992, 1993), and Chen *et al.* (1989) used lithium chloride (LiCl); Ullah *et al.* (1988), Kinsara *et al.* (1998) and Lazzarin *et al.* (1999) used calcium chloride (CaCl₂); while Ahmed *et al.* (1997) and Patnaik *et al.* (1990) used lithium bromide (LiBr). Other experiments for absorbers using LiCl were carried out by Kessling *et al.* (1998), Kim *et al.* (1997) and Scalabrin and Scaltriti (1990).

The moisture that transfers from the air to the liquid desiccant in the dehumidifier causes a dilution of the desiccant resulting in a reduction in its ability to absorb more water. Therefore, the desiccant must be regenerated to its original concentration. The regeneration process requires heat which can be obtained from a low temperature source, for which solar energy and waste energy from other processes are suitable. Different ways to regenerate liquid desiccants have been proposed. Hollands (1963) presented results from the regeneration of lithium chloride in a solar still. Hollands focused his study on the still efficiency, concluding that lithium chloride can be regenerated in a solar still with a daily efficiency of 5 to 20% depending on the insolation and the concentration of the desiccant. Ahmed Khalid *et al.* (1998) presented an exergy analysis of a partly closed solar generator to compare it with the solar collector reported previously. Ahmed *et al.* (1997) simulated a hybrid cycle with a partly closed-open solar regenerator for regenerating the weak solution. They found that the system COP is about 50% higher than that of a conventional vapor absorption machine. Leboeuf and Löf (1980) presented an analysis of a lithium chloride open cycle absorption air conditioner which utilizes a packed bed for regeneration of the desiccant solution driven by solar heated air. In this case, the air temperature ranged from 65 to 96°C while the desiccant temperature ranged from 40 to 55°C. Löf *et al.* (1984) conducted experimental and theoretical studies of regeneration of aqueous lithium chloride solution with solar heated air in a packed column. In this case, air at a temperature of 82 to 109°C was used to regenerate the desiccant at an average temperature of 36°C.

In any thermodynamic system, the conditions of the working fluids and parameters of the physical equipment define the overall performance of the system. In a liquid desiccant cooling system, variables such as air and desiccant flow rate, air temperature and humidity, desiccant temperature and concentration are of great interest for the performance of the dehumidifier. The mass ratio of air to desiccant solution $MR = \dot{m}_{\text{air}} / \dot{m}_{\text{sol}}$

is an important factor for absorber efficiency and system capacity. Previous studies have reported the performance of packed bed absorbers and regenerators with MR between 1.3 and 3.3. The range of MR varies with the type of absorber/regenerator, but in general better results are obtained for small MR.

For simulation purposes, validated models are required for modeling the absorber in a liquid desiccant system. Models using lithium chloride have been described by Khan and Martinez (1998), Ahmed *et al.* (1997) and Kavasogullari *et al.* (1991). Due to the complexity of the dehumidification process, theoretical modeling relies heavily upon experimental data. Öberg and Goswami (1998b) developed a model for a packed bed liquid desiccant air dehumidifier and regenerator with triethylene glycol as liquid desiccant which was validated satisfactorily by the experimental data. The present study uses a modified version of the mathematical model developed by Öberg and Goswami to compare the experimental results of a packed bed dehumidifier and regenerator using lithium chloride as a desiccant.

2. EXPERIMENTAL FACILITY AND PROCEDURE

A schematic of the experimental facility is shown in Fig. 1. The packed bed absorption tower was constructed from a 25.4 cm (24 cm I.D.) diameter acrylic tube to allow for flow visualization. The height of the tower is constant and equal to 60 cm. The packings used were 2.54 cm (1 in.) polypropylene Rauschert Hiflow[®] rings with specific surface area of 210 m²/m³. Fresh, unused lithium chloride was stored in a tank, and its temperature was adjusted by circulating cold or warm water through a submerged stainless steel coil. Air was blown past an air heater or a cooling coil, and through a humidifying chamber to adjust its temperature and relative humidity before it enters the packed tower. When the desired air and desiccant conditions were obtained, the desiccant was allowed to flow through the tower. The desiccant was distributed over the packings by three spray heads evenly spaced in an equilateral triangular configuration.

Once steady state was obtained, measurements were taken using a PC-based data acquisition system. These measurements included inlet and outlet temperatures of the desiccant and the air using copper-constantan thermocouples, as well as inlet and outlet air relative humidities using

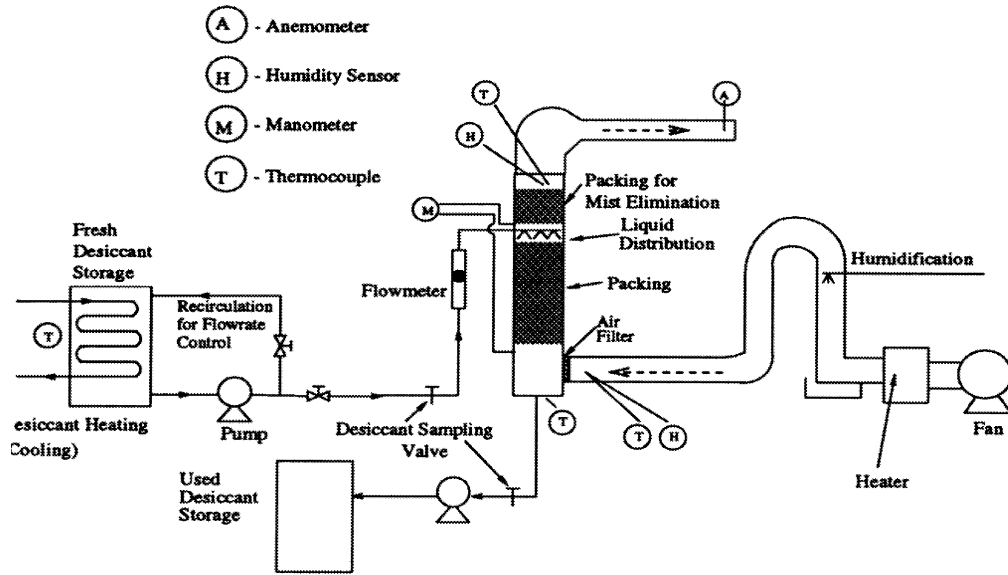


Fig. 1. Experimental facility.

humidity probes. In addition, samples of the desiccant entering the dehumidifier were taken during the experiment and analyzed for water content using Karl Fischer titration. To study dehumidification, the rate of moisture removal from the air (water condensation rate) was studied experimentally as a function of the following variables: air and desiccant flow rates; air temperature and humidity ratio; and desiccant temperature and concentration. To study the regeneration process, experiments were undertaken to study the rate of water evaporation from the liquid desiccant as a function of the above variables. For the same variables an analysis of the tower efficiency was done using humidity effectiveness. Experiments were conducted for each variable at three levels (low, intermediate, and high value) while keeping the other variables constant. Three experiments were conducted at each level, and an average was used in the results.

3. THEORETICAL HEAT AND MASS TRANSFER MODEL OF THE PACKED BED TOWER

Öberg and Goswami (1998b) developed a finite difference model based on the model for adiabatic gas absorption presented by Treybal (1969) with the exception that the resistance to heat transfer in the liquid phase was neglected. For their model they assumed adiabatic absorption; concentration and temperature gradients in the flow direction (Z -direction, referring to Fig. 2) only; only water is transferred between the air and the desiccant;

the interfacial surface area is the same for heat transfer and mass transfer, and equal to the specific surface area of the packings; the heat of mixing is negligible as compared to the latent heat of condensation of the water; and the resistance to heat transfer in the liquid phase is negligible. For the finite difference model, the packed bed height Z is divided into small segments, dZ (Fig. 2b), and the mass and energy balances are solved for each segment, from the bottom to the top of the tower. Since only the inlet conditions of the desiccant are known, the outlet conditions must initially be guessed, and iterations are required to find the desiccant outlet conditions that give the known inlet conditions at the top of the packed bed.

Öberg and Goswami's finite difference model, which worked well for TEG as the desiccant,

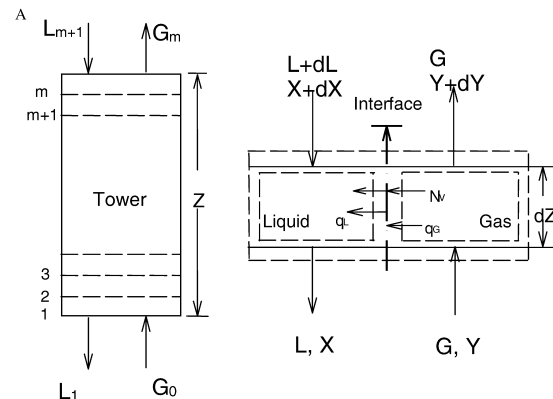


Fig. 2. Packed bed dehumidifier: (a) overview; (b) differential segment.

required two modifications to account for the higher surface tension of LiCl and higher water concentration in brines as compared to water concentration in TEG. The modifications and governing equations that describe the changes in air humidity and air temperature, desiccant temperature and desiccant concentration, and desiccant flow rate across a segment are given below.

Öberg and Goswami assumed that the interfacial surface area is the same for heat and mass transfer, and is equal to the specific surface area of the packing. Because of the high surface tension of LiCl solutions (twice that of glycol) the packing is wetted insufficiently causing a considerable reduction of the area for mass transfer. Therefore, to estimate the wet area, an equation for wetted surface area proposed by Onda *et al.* (1968) was used:

$$\frac{a_w}{a_t} = 1 - \exp \left[-1.45 \left(\frac{\gamma_L}{\gamma_L} \right)^{0.75} \left(\frac{L}{a_t \cdot \mu_L} \right)^{0.1} \left(\frac{L^2 \cdot a_t}{\rho_L^2 \cdot g} \right)^{-0.05} \left(\frac{L^2}{\rho_L \cdot \gamma_L \cdot a_t} \right)^{0.2} \right] \quad (1)$$

This equation takes into account the liquid surface tension and the surface energy of packing materials, and was used by Öberg and Goswami in the definition of k -type mass transfer coefficients:

$$k_L = 0.0051 \left(\frac{\mu_L \cdot g}{\rho_L} \right)^{1/3} \left(\frac{L}{a_w \cdot \mu_L} \right)^{2/3} \left(\frac{\rho_L \cdot D_L}{\mu_L} \right)^{1/2} (a_t \cdot D_p)^{0.4} \quad (2)$$

$$k_G = 5.23 \frac{a_t \cdot D_G}{R \cdot T_a} \left(\frac{G}{a_t \cdot \mu_G} \right)^{0.7} \left(\frac{\mu_G}{\rho_G \cdot D_G} \right)^{1/3} (a_t \cdot D_p)^{-2} \quad (3)$$

Then, the change in air humidity across a differential segment is defined by:

$$\frac{dY}{dZ} = - \frac{M_w \cdot F_G \cdot a_w}{G} \cdot \ln \left(\frac{1 - y_i}{1 - y} \right) \quad (4)$$

where the interfacial gas phase concentration is given by:

$$y_i = 1 - (1 - y) \cdot \left(\frac{x}{x_i} \right)^{F_L/F_G} \quad (5)$$

Eq. (5) was used with the vapor–liquid equilibrium curve for LiCl to solve for the interfacial concentrations in the gas and liquid phases.

The k -type mass transfer coefficients for liquid phase can be converted to F -type coefficients by:

$$F_L = k_L \cdot x_{SM} \cdot \frac{\rho_L}{M_L} \quad (6)$$

where x_{SM} may be considered equal to 1 for very

dilute solutions. For lithium chloride the logarithmic mean desiccant mole fraction difference between the bulk liquid and interface values must be calculated as:

$$x_{SM} = \frac{x - x_i}{\ln(x/x_i)} \quad (7)$$

and the k -type mass transfer coefficient for gas phase can be converted to F -type coefficients by:

$$F_G = k_G \cdot P \quad (8)$$

The change in air temperature across the differential segment is given by:

$$\frac{dT_a}{dZ} = \frac{h'_G a_t \cdot (T_L - T_a)}{G \cdot (c_{p,a} + Y \cdot c_{p,v})} \quad (9)$$

where $h'_G a_t$ is the heat transfer coefficient corrected for simultaneous heat and mass transfer:

$$h'_G a_t = \frac{-G \cdot c_{p,v} \cdot \frac{dY}{dZ}}{1 - \exp \left(\frac{G \cdot c_{p,v} \cdot \frac{dY}{dZ}}{h_G \cdot a_t} \right)} \quad (10)$$

and applying the heat and mass transfer analogy, it is found that the gas phase heat transfer coefficient is:

$$h_G = F_G \cdot M_a \cdot (C_{p,a} + Y \cdot C_{p,v}) \cdot \frac{Sc^{2/3}}{Pr^{2/3}} \quad (11)$$

with $Sc = \mu_G / (\rho_G \cdot D_G)$.

The change in desiccant flow rate, concentration and temperature across the differential segment are given by Eqs. (12), (13) and (14), respectively:

$$\frac{dL}{dZ} = G \cdot \frac{dY}{dZ} \quad (12)$$

$$\frac{dX}{dZ} = - \frac{G}{L} \cdot X \cdot \frac{dY}{dZ} \quad (13)$$

$$\frac{dT_L}{dZ} = \frac{G}{c_{p,L} \cdot L} \left\{ (c_{p,a} + Y \cdot c_{p,v}) \frac{dT_a}{dZ} + [c_{p,v} \cdot (T_a - T_o) - c_{p,L} (T_L - T_o) + \lambda_o] \frac{dY}{dZ} \right\} \quad (14)$$

Vapor pressure is an important property which determines the air humidity ratio in equilibrium with the desiccant at the interface. In this study, a second order polynomial was used and the coefficients were obtained from a curve fit using data from Uemura (1967):

$$\begin{aligned}
p_V = & (a_o + a_1 \cdot T + a_2 \cdot T^2) \\
& + (b_o + b_1 \cdot T + b_2 \cdot T^2) \cdot X \\
& + (c_o + c_1 \cdot T + c_2 \cdot T^2) \cdot X^2
\end{aligned} \quad (15)$$

where the constants are given for the dehumidification process as:

$$\begin{aligned}
a_o &= 4.58208, & a_1 &= -0.159174, \\
a_2 &= 0.0072594, & b_o &= -18.3816, \\
b_1 &= 0.5661, & b_2 &= -0.019314 \\
c_o &= 21.312, & c_1 &= -0.666, & c_2 &= 0.01332; \\
T & (\text{°C}), & X & (\text{kg}_{\text{LiCl}}/\text{kg}_{\text{sol}}),
\end{aligned}$$

and for the regeneration process as:

$$\begin{aligned}
a_o &= 16.294, & a_1 &= -0.8893, & a_2 &= 0.01927, \\
b_o &= 74.3, & b_1 &= -1.8035, & b_2 &= -0.01875 \\
c_o &= -226.4, & c_1 &= 7.49, & c_2 &= -0.039; \\
T & (\text{°C}), & X & (\text{kg}_{\text{LiCl}}/\text{kg}_{\text{sol}}).
\end{aligned}$$

A sensitivity analysis comparing the data from Uemura (1967), and Zaytsev and Aseyev (1992) has shown that the deviation of the results obtained from the mathematical model can be of the order of 11%.

The efficiency of the tower was evaluated through a humidity effectiveness defined for the dehumidifier as:

$$\epsilon_Y = \frac{Y_{\text{IN}} - Y_{\text{OUT}}}{Y_{\text{IN}} - Y_{\text{equ}}} \quad (16)$$

and for the regenerator as:

$$\epsilon_Y = \frac{Y_{\text{OUT}} - Y_{\text{IN}}}{Y_{\text{equ}} - Y_{\text{IN}}} \quad (17)$$

For this relation, Y_{IN} and Y_{OUT} are the humidity ratios of the air at the inlet and outlet of the tower, respectively. Y_{equ} is the humidity ratio of the air, which is in equilibrium with the desiccant solu-

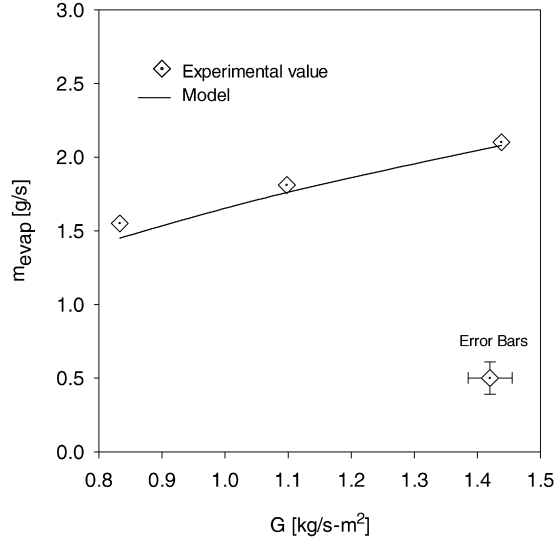


Fig. 3. Influence of air flow rate on dehumidification.

tion at the local solution temperature and concentration.

An additional consideration was introduced in the model to account for the non-uniform liquid distribution at the top of the tower. The packing volume that is dry is estimated by using geometric relations allowing the calculation of a correction factor for unwetted packing fraction, CF. This correction factor was used to modify the relation a_w/a_t in Eq. (1), as $a_w/(a_t \cdot \text{CF})$.

4. RESULTS AND DISCUSSION

4.1. Air dehumidification

Table 1 presents the experimental results, while Figs. 3–8 show the experimental results for dehumidification together with the theoretical modeling results. Uncertainties of the experimen-

Table 1. Air dehumidification experimental results

| Inlet | | | | | | Outlet | | | | m_{cond} |
|-------|-------|--------|-------|-------|------|--------|--------|-------|------|-------------------|
| G | T_a | Y | L | T_L | X | T_a | Y | T_L | X | |
| 0.890 | 30.1 | 0.0180 | 6.124 | 30.1 | 34.6 | 31.3 | 0.0104 | 32.3 | 34.5 | 0.32 |
| 1.180 | 30.1 | 0.0181 | 6.227 | 30.3 | 34.7 | 32.2 | 0.0108 | 32.6 | 34.6 | 0.40 |
| 1.513 | 30.2 | 0.0181 | 6.113 | 30.0 | 34.3 | 32.2 | 0.0108 | 32.7 | 34.1 | 0.52 |
| 1.189 | 35.5 | 0.0188 | 6.290 | 30.3 | 34.5 | 32.8 | 0.0112 | 32.6 | 33.7 | 0.42 |
| 1.183 | 40.1 | 0.0180 | 6.287 | 30.5 | 34.4 | 33.1 | 0.0115 | 32.9 | 34.3 | 0.36 |
| 1.214 | 30.3 | 0.0142 | 6.273 | 30.1 | 33.9 | 31.1 | 0.0103 | 31.5 | 33.8 | 0.23 |
| 1.187 | 29.9 | 0.0215 | 6.272 | 30.3 | 33.9 | 33.4 | 0.0120 | 33.1 | 33.7 | 0.53 |
| 1.190 | 30.1 | 0.0180 | 5.019 | 30.2 | 34.4 | 32.2 | 0.0113 | 32.7 | 34.2 | 0.38 |
| 1.182 | 30.2 | 0.0181 | 7.420 | 30.2 | 34.4 | 32.0 | 0.0110 | 32.5 | 34.3 | 0.39 |
| 1.198 | 29.9 | 0.0177 | 6.269 | 25.0 | 34.7 | 28.2 | 0.0088 | 28.4 | 34.5 | 0.50 |
| 1.176 | 29.9 | 0.0178 | 6.309 | 35.2 | 34.9 | 35.7 | 0.0140 | 36.2 | 34.8 | 0.21 |
| 1.182 | 29.9 | 0.0179 | 6.164 | 30.1 | 33.1 | 32.4 | 0.0114 | 32.2 | 33.0 | 0.36 |
| 1.192 | 29.9 | 0.0179 | 6.267 | 30.2 | 33.8 | 32.5 | 0.0112 | 32.6 | 33.7 | 0.38 |
| 1.176 | 30.0 | 0.0181 | 6.206 | 30.2 | 34.8 | 32.0 | 0.0107 | 32.5 | 34.7 | 0.41 |

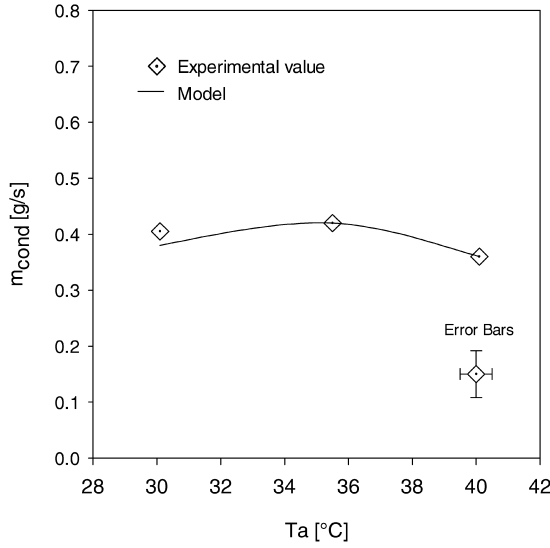


Fig. 4. Influence of inlet air temperature on dehumidification.

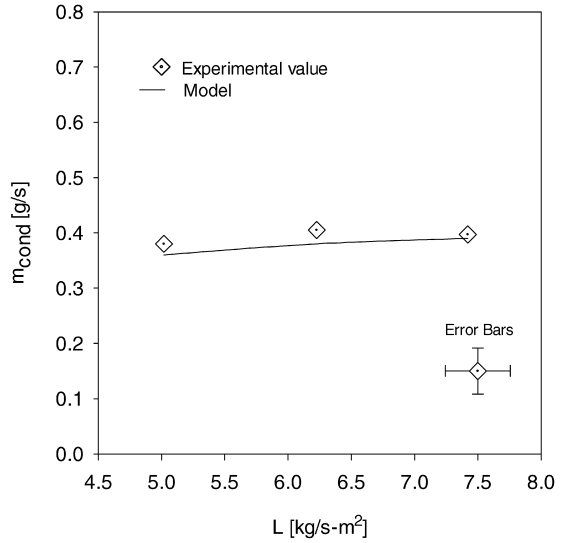


Fig. 6. Influence of desiccant flow rate on dehumidification.

tal measurements were calculated using the method by Kline and McClinton (1953). Error bars obtained from these calculations are also shown in the figures. It is seen from the figures that the adapted finite difference model shows very good agreement with the experimental findings. The variables found to have the most significant effect on the dehumidifier performance are: air flow rate, humidity ratio, desiccant temperature, and desiccant concentration. Figs. 3–8 show that the influence of these variables may be assumed linear. Therefore, the slope of the condensation rate curve (% change in m_{cond} /% change in variable) in these figures gives an estimation of

the influence of these variables on the water condensation rate. The water condensation rate increases with the air flow rate with a slope of 0.9 (Fig. 3). It may be explained that a high air flow rate will remove the dehumidified air more rapidly from the interface, thereby reducing the humidity gradient between the interface and bulk air, and maintaining a higher potential for mass transfer. The water condensation rate increases with the inlet air humidity ratio with a slope of 2.5 (Fig. 5). It happens because a higher humidity ratio implies a higher air vapor pressure and consequently higher potential for mass transfer. The water condensation rate decreases with the desiccant temperature with a slope of -1.4 (Fig.

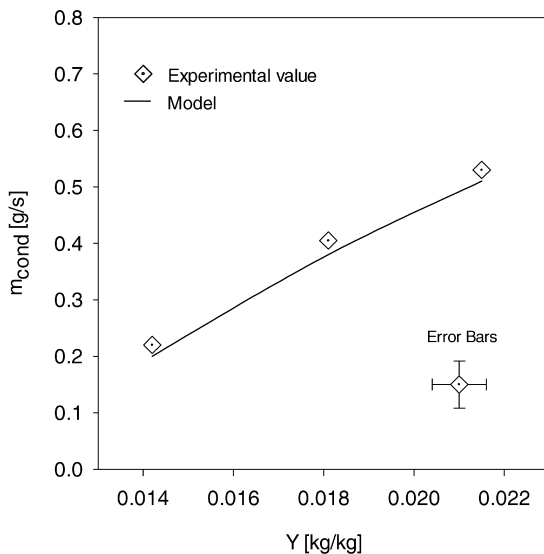


Fig. 5. Influence of inlet air humidity ratio on dehumidification.

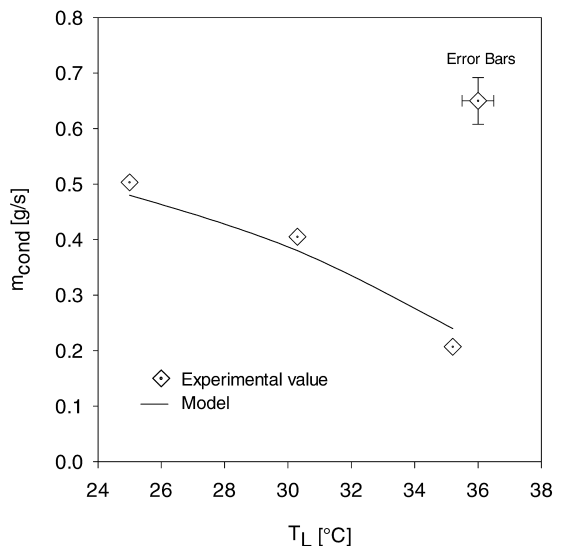


Fig. 7. Influence of inlet desiccant temperature on dehumidification.

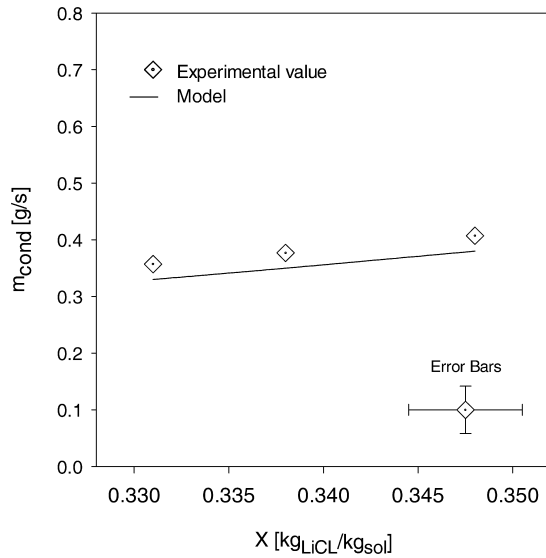


Fig. 8. Influence of inlet desiccant concentration on dehumidification.

7). A higher desiccant temperature gives a lower potential for mass transfer in the dehumidifier resulting in a lower condensation rate. The water condensation rate increases with the desiccant concentration with a slope of 2.7 (Fig. 8). A higher desiccant concentration gives a higher potential for mass transfer in the dehumidifier resulting in a greater condensation rate. It may be pointed out that if the air temperature is considerably higher than the desiccant temperature, the desiccant temperature will increase, resulting in a reduction in the potential for mass transfer (Fig. 4). The desiccant flow rate does not cause significant variation in the water condensation rate (Fig. 6); however, the liquid flow rate must be high enough to ensure wetting of the packing. For the range of the variables studied, humidity effectiveness for the absorber remains mostly stable, no variation higher than 6% was found.

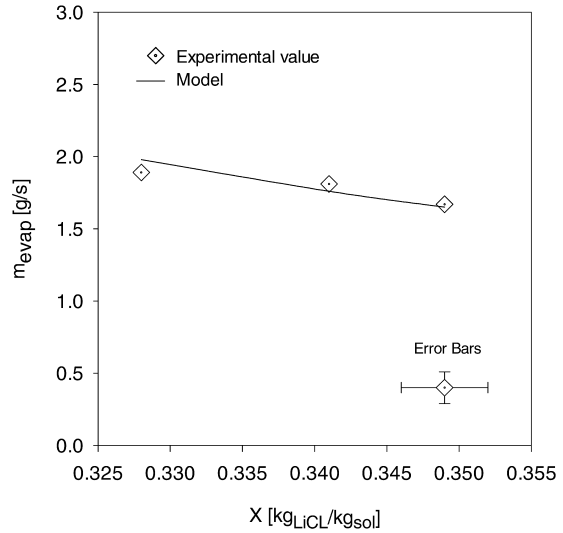


Fig. 9. Influence of air flow rate on desiccant regeneration.

The only clear trends observed were: slight decrease of the humidity effectiveness with air flow rate and air temperature; and slight increase of the humidity effectiveness with desiccant flow rate. The lower value of humidity effectiveness was 75% and the higher 84%.

4.2. Regeneration

Table 2 presents the experimental results for regeneration, while Figs. 9–14 show the experimental results together with the theoretical modeling. These figures show that the influence of the variables may be assumed linear. Therefore, the slope of the evaporation rate curve (% change in m_{evap} /% change in variable) in these figures gives an estimation of the influence of these variables on the water evaporation rate. The water evaporation rate increases with the air flow rate with a slope of 0.5 (Fig. 9). Since a high air flow rate rapidly removes the higher moist air from the

Table 2. Regeneration experimental results

| Inlet | | | | | | Outlet | | | | m_{evap} |
|-------|-------|--------|-------|-------|------|--------|--------|-------|------|------------|
| G | T_a | Y | L | T_L | X | T_a | Y | T_L | X | |
| 0.833 | 30.4 | 0.0183 | 6.463 | 65.0 | 34.0 | 58.9 | 0.0579 | 58.6 | 34.5 | 1.55 |
| 1.098 | 30.1 | 0.0180 | 6.206 | 65.1 | 34.1 | 59.3 | 0.0532 | 57.8 | 34.8 | 1.81 |
| 1.438 | 29.8 | 0.0177 | 6.479 | 65.1 | 34.5 | 57.5 | 0.0488 | 56.6 | 35.2 | 2.10 |
| 1.097 | 35.1 | 0.0180 | 6.349 | 65.1 | 33.4 | 58.5 | 0.0551 | 57.4 | 34.1 | 1.91 |
| 1.102 | 40.0 | 0.0178 | 6.354 | 65.0 | 33.6 | 58.9 | 0.0548 | 57.6 | 34.2 | 1.91 |
| 1.132 | 30.2 | 0.0143 | 6.370 | 65.2 | 34.0 | 57.6 | 0.0513 | 57.2 | 34.7 | 1.97 |
| 1.097 | 29.4 | 0.0210 | 6.440 | 65.5 | 33.6 | 58.5 | 0.0541 | 58.3 | 34.2 | 1.70 |
| 1.116 | 30.3 | 0.0182 | 5.185 | 65.4 | 34.4 | 57.6 | 0.0507 | 57.0 | 34.9 | 1.71 |
| 1.101 | 29.9 | 0.0180 | 7.541 | 65.2 | 34.3 | 59.0 | 0.0556 | 57.9 | 34.9 | 1.95 |
| 1.111 | 30.0 | 0.0187 | 6.245 | 60.3 | 34.4 | 55.8 | 0.0447 | 54.2 | 34.8 | 1.36 |
| 1.084 | 29.7 | 0.0184 | 6.315 | 70.0 | 34.5 | 62.6 | 0.0666 | 60.0 | 35.3 | 2.45 |
| 1.099 | 29.7 | 0.0177 | 6.400 | 64.8 | 32.8 | 57.6 | 0.0542 | 56.8 | 33.4 | 1.89 |
| 1.116 | 30.3 | 0.0182 | 6.428 | 65.0 | 34.9 | 57.9 | 0.0501 | 57.5 | 35.4 | 1.67 |

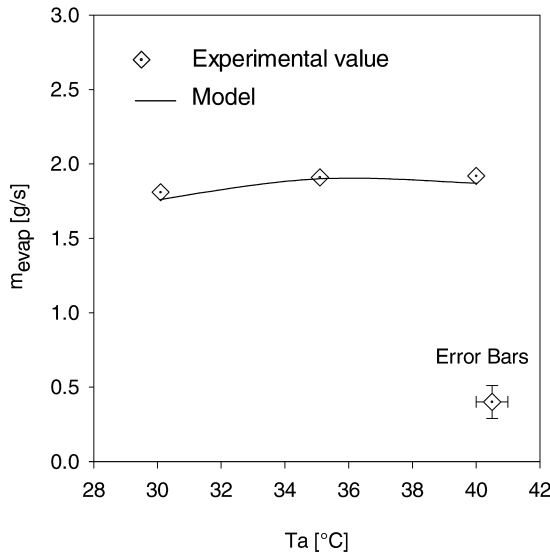


Fig. 10. Influence of inlet air temperature on desiccant regeneration.

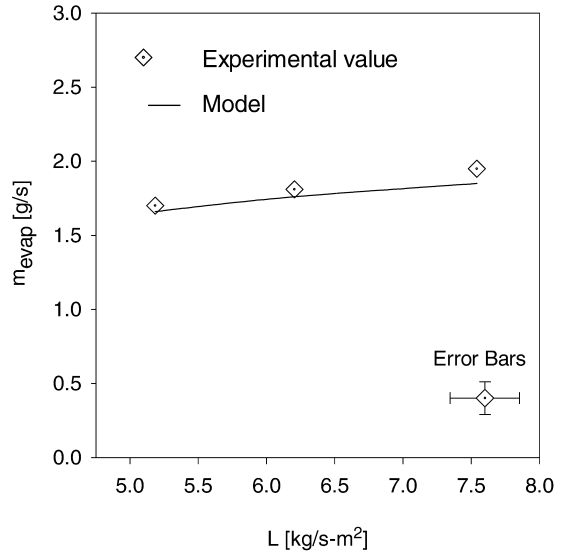


Fig. 12. Influence of desiccant flow rate on desiccant regeneration.

interface, it reduces the humidity gradient between the interface and bulk air, maintaining a higher potential for mass transfer. The water evaporation rate increases with the inlet desiccant temperature with a slope of 5 (Fig. 13). Since vapor pressure of the desiccant is highly dependent on the temperature, the higher the temperature the higher the vapor pressure, and consequently higher the potential for mass transfer. The water evaporation rate decreases with the inlet desiccant concentration with a slope of -1.8 (Fig. 14). This may be explained from the fact that vapor pressure of the desiccant is a function

of the concentration. Therefore, the higher the concentration, the lower the vapor pressure, and consequently the lower the potential for mass transfer. The water evaporation rate decreases with the inlet air humidity ratio with a slope of -0.3 (Fig. 11). As expected, a higher humidity ratio implies higher air vapor pressure and consequently lower potential for mass transfer. The water evaporation rate increases with the desiccant flow rate with a slope of 0.3 (Fig. 12). At higher desiccant flow rates there will be less reduction of the liquid temperature, maintaining a higher potential for mass transfer. The air tem-

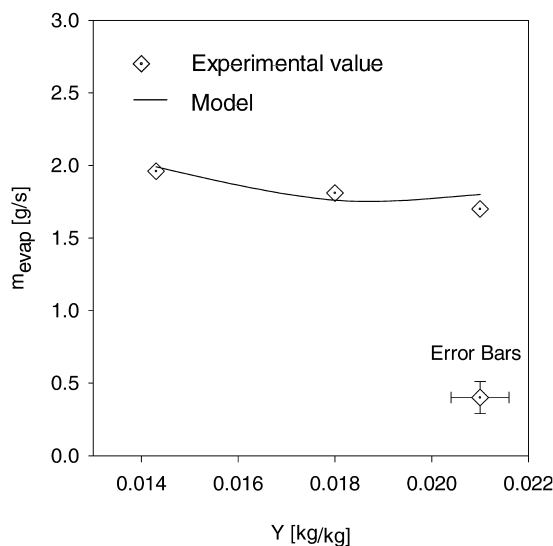


Fig. 11. Influence of inlet air humidity ratio on desiccant regeneration.

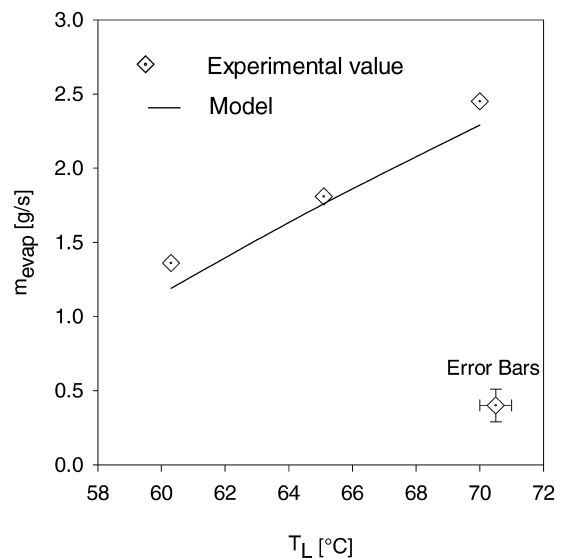


Fig. 13. Influence of inlet desiccant temperature on desiccant regeneration.

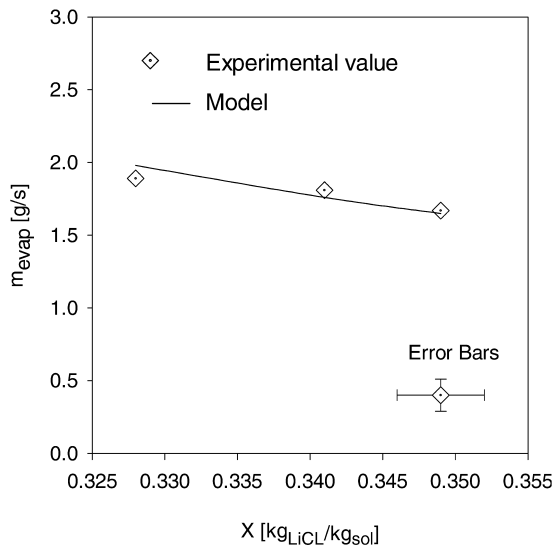


Fig. 14. Influence of inlet desiccant concentration on desiccant regeneration.

perature does not cause significant variation in the water evaporation rate (Fig. 10).

Efficiency of the regenerator is more sensitive than that of the dehumidifier. For the range of the variables studied, humidity effectiveness for the regenerator varies between 71 and 87%. Two defined tendencies were noticed from the results. One tendency is the apparent linear decrease of

the humidity effectiveness for an increase in the air flow rate. This can be explained because for a higher air flow rate the air will be in contact with the liquid for a shorter period of time, giving a lower change in air humidity ratio (Fig. 15). The second defined tendency is the apparent linear increase of humidity effectiveness with the increase of desiccant flow rate. This can be explained from the result seen earlier that the water evaporation rate is proportional to the desiccant flow rate. Therefore, for a higher desiccant flow rate, the change in air humidity ratio will be higher (Fig. 16).

5. CONCLUSIONS

Reliable sets of data for air dehumidification and desiccant regeneration using lithium chloride were obtained. The influence of the design variables studied on the water condensation rate from the air and evaporation rate from the desiccant can be assumed linear. Therefore, the slope of the curves in Figs. 3–14 give a measurement of the impact of the variable on the water condensation and evaporation rates. Design variables found to have the greatest impact on the performance of the dehumidifier are: desiccant concentration (slope=2.7), desiccant temperature (slope=−1.4), air flow rate (slope=−0.9), and air hum-

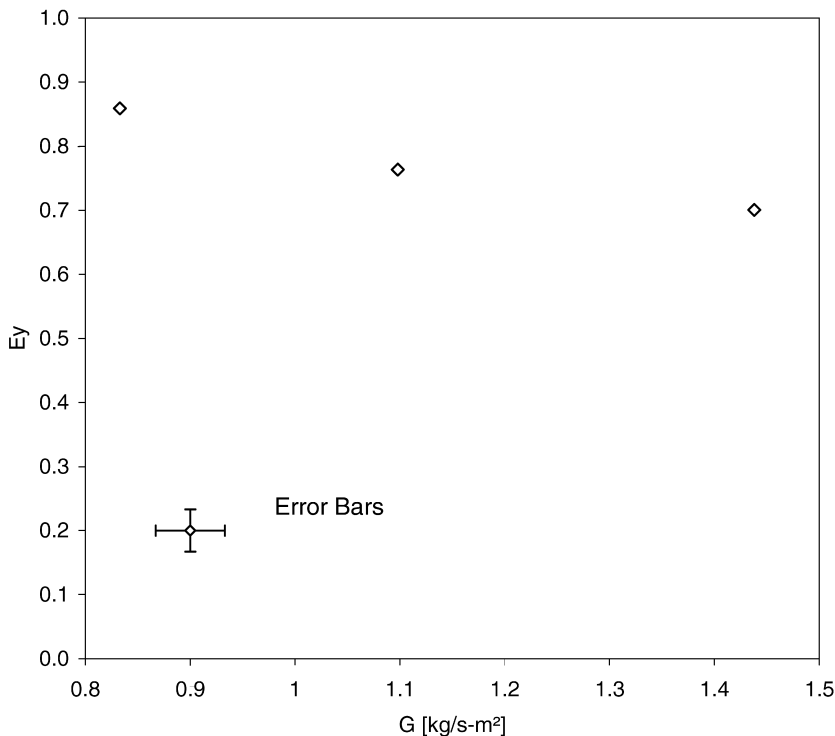


Fig. 15. Influence of air flow rate on humidity effectiveness.

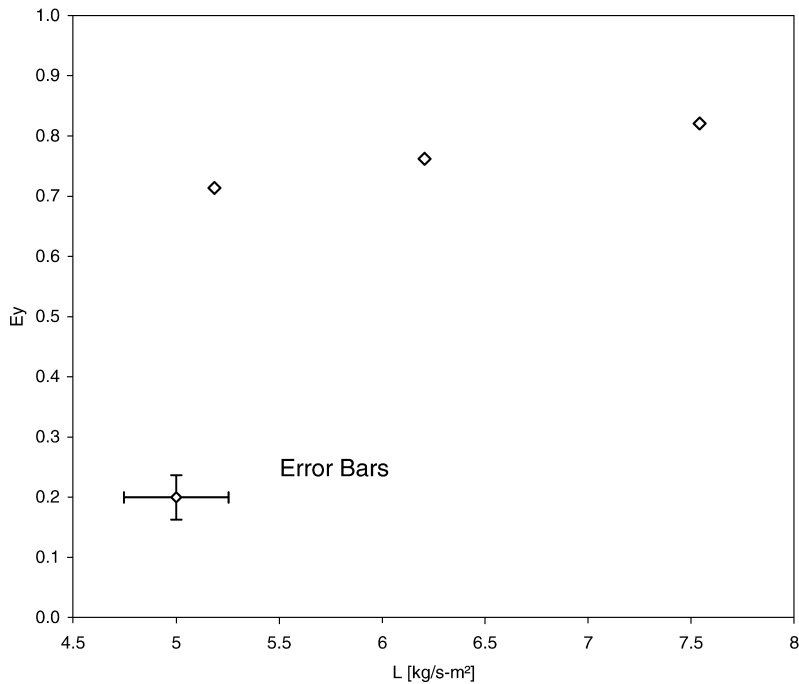


Fig. 16. Influence of desiccant flow rate on humidity effectiveness.

idity ratio (slope=2.5). Design variables found to have the greatest impact on the performance of the regenerator are: desiccant temperature (slope=5), desiccant concentration (slope=-1.8), air flow rate (slope=0.5). The other variables have a slope equal or lower than 0.3. In this study the mass flow ratio of air to desiccant solution (MR) varied between 0.15 and 0.25 for both the air dehumidification and desiccant regeneration experiments, which is lower than the MR values of 1.3 to 3.3 used in most other studies. The adapted finite difference model shows very good agreement with the experimental findings.

NOMENCLATURE

| | |
|-------|--|
| a_t | specific surface area of packing (m ² /m ³) |
| a_w | wetted surface area of packing (m ² /m ³) |
| c_p | specific heat (kJ/kg °C) |
| D | diffusivity (m ² /s) |
| D_p | nominal size of packing (m) |
| F_G | gas phase mass transfer coefficient (kmol/m ² s) |
| F_L | liquid phase mass transfer coefficient (kmol/m ² s) |
| G | superficial air (gas) flow rate (kg/m ² s) |
| g | acceleration of gravity (m/s ²) |
| h_G | gas side heat transfer coefficient (kJ/m ² s) |
| k_G | gas phase mass transfer coefficient (kmol/m ² s Pa) |
| k_L | liquid phase mass transfer coefficient (m/s) |
| L | superficial desiccant flow rate (kg/m ² s) |
| LiCl | lithium chloride |
| M | molar mass (kg/kmol) |

| | |
|----------|--|
| m | flow rate (g/s) or (kg/s) |
| P | total pressure (Pa) |
| Pr | Prandtl number |
| p_v | vapor pressure (Pa) |
| Sc | Schmidt number |
| T | temperature (°C) |
| X | desiccant concentration (kg _{LiCl} /kg _{solution}) |
| x | desiccant mole fraction (kmol _{LiCl} /kmol _{solution}) |
| x_{SM} | logarithmic mean solvent mole fraction difference between the bulk liquid and interface values (kmol _{LiCl} /kmol _{solution}) |
| Y | air humidity ratio (kg water/kg dry air) |
| y | water mole fraction (kmol water/kmol air) |
| Z | tower height (m) |

Greek letters

| | |
|------------|-------------------------------------|
| γ | surface tension (N/m) |
| ϵ | effectiveness |
| λ | latent heat of condensation (kJ/kg) |
| μ | viscosity (N/m ²) |
| ρ | density (kg/m ³) |

Subscripts

| | |
|------|---------------------------|
| a | air |
| c | critical |
| cond | water condensation |
| equ | equivalent |
| evap | water evaporation |
| G | gas phase |
| IN | inlet |
| i | interface |
| L | desiccant or liquid phase |
| OUT | outlet |
| o | reference state |

REFERENCES

- Ahmed K. S., Gandhidasan P. and Al-Farayedhi A. A. (1997) Simulation of a hybrid liquid desiccant based air-conditioning system. *Appl. Thermal Eng.* **17**(2), 125–134.
- Ahmed Khalid C. S., Gandhidasan P., Zubair S. M. and Al-Farayedhi A. A. (1998) Exergy analysis of a liquid desiccant based air-conditioning system. *Energy* **23**(1), 51–59.
- Burns P. R., Mitchell J. W. and Beckman W. A. (1985) Hybrid desiccant cooling system in supermarket applications. *ASHRAE Trans.* **91**(pt. 1b), 457–468.
- Chen L. C., Kuo C. L. and Shyu R. J. (1989) The performance of a packed bed dehumidifier for solar liquid desiccant system. *Proceedings of the 11th Annual ASME Solar Energy Conference*, San Diego, California, pp. 371–377.
- Chengchao F. and Ketao S. (1997) Analysis and modeling of solar liquid desiccant air conditioning system. *Taiyanneng Xuebao/Acta Energetica Sinica* **18**(2), 128–133.
- Chung T. W., Ghosh T. K. and Hines A. L. (1993) Dehumidification of air by aqueous lithium chloride in a packed column. *Sep. Sci. Technol.* **28**(1–3), 533–550.
- Chung T. W., Ghosh T. K. and Hines A. L. (1992) Mass and heat transfer coefficients for water absorption by lithium chloride. *Inst. Chem. Eng. Symp. Ser.* **2**(128), B43–B53.
- Hollands K. G. T. (1963) The regeneration of lithium chloride brine in a solar still. *Solar Energy* **7**(2), 39–43.
- Kavasogullari S., Gandhidasan P., Ertas A. and Anderson E. (1991) Performance of CaCl₂ and LiCl liquid desiccants in a dehumidifying packed tower. *ASME Emerg. Technol.* **36**, 45–49.
- Kessling W., Laevermann E. and Kapfhammer C. (1998) Energy storage for desiccant cooling systems component developed. *Solar Energy* **64**(4–6), 209–221.
- Khan A. Y. and Martinez J. (1998) Modeling and parametric analysis of heat and mass transfer performance of a hybrid liquid desiccant absorber. *Energy Convers. Manage.* **39**(10), 1095–1112.
- Kim K. J., Ameen T. A. and Wood B. D. (1997) Performance evaluations of LiCl and LiBr for absorber design applications in the open-cycle absorption refrigeration system. *J. Solar Energy Eng.* **119**(2), 165–173.
- Kinsara A. A., Al-Rabghi O. and Elsayed M. M. (1998) Parametric study of an energy efficient air conditioning system using liquid desiccant. *Appl. Thermal Eng.* **18**(5), 327–335.
- Kline S. J. and McClinton F. A. (1953) Uncertainties in single-sample experiments. *Mech. Eng.* **75**, 3–8.
- Lazzarin R., Gasparlla A. and Longo G. (1999) Chemical dehumidification by liquid desiccant: theory and experiment. *Int. J. Refrig.–Revue Internationale Du Froid* **22**(4), 334–347.
- Leboeuf C. M. and Löf G. O. G. (1980) Open-cycle absorption cooling using packed-bed absorbent reconcentration. *Proceedings of the Annual Meeting of the American Section of the International Solar Energy Society, AS/ISES* **Vol. 3**(1), 205–209a.
- Löf G. O. G., Lenz T. G. and Rao S. (1984) Coefficients of heat and mass transfer in a packed bed suitable for solar regeneration of aqueous lithium chloride solutions. *J. Solar Energy Eng.* **106**, 387–392.
- Öberg V. and Goswami D. Y. (1998a) Performance simulation of solar hybrid liquid desiccant cooling for ventilation air preconditioning. In *Solar Engineering 1998, Proceedings of the International Solar Energy Engineering Conference*, pp. 176–182, ASME, Fairfield, NJ.
- Öberg V. and Goswami D. Y. (1998b) Experimental study of the heat and mass transfer in a packed bed liquid desiccant air dehumidifier. *J. Solar Energy Eng. Trans. ASME* **120**, 289–297.
- Öberg V. and Goswami D. Y. (1998c) A review of liquid desiccant cooling. In *Advances in Solar Energy*, Vol. 12, Böer K. W. (Ed.), pp. 431–470, ASES, Boulder, CO.
- Onda K., Takeuchi H. and Olumoto Y. (1968) Mass transfer coefficients between gas and liquid phases in packed columns. *Journal of Chemical Engineering of Japan* **1**(1), 56–62.
- Patnaik S., Lenz T. G. and Löf G. O. G. (1990) Performance studies for an experimental solar open-cycle liquid desiccant air dehumidification system. *Solar Energy* **44**, 123–135.
- Scalabrin G. and Scaltriti G. (1990) A liquid sorption–desorption system for air conditioning with heat at lower temperature. *ASME J. Solar Energy Eng.* **112**, 70–75.
- Treybal R. E. (1969). In 3rd edn., *Mass Transfer Operations*, McGraw-Hill, New York.
- Uemura T. (1967) Studies on the lithium chloride–water absorption refrigeration machine. In *Technology Reports of Kansai University*, No. 9, pp. 71–84.
- Ullah M. R., Kettleborough C. F. and Gandhidasan P. (1988) Effectiveness of moisture removal for an adiabatic counterflow packed tower absorber operating with CaCl₂–air contact system. *ASME J. Solar Energy Eng.* **110**, 98–101.
- Zaytsev I. D. and Aseyev G. G. (1992). *Properties of Aqueous Solutions of Electrolytes*, CRC Press, Boca Raton.